Case Studies in Structural Engineering 5 (2016) 1–12

Contents lists available at ScienceDirect

Case Studies in Structural Engineering

journal homepage: www.elsevier.com/locate/csse

Short communication

Efficient masonry vault inspection by Monte Carlo simulations: Case of hidden defect

Abdelmounaim Zanaz[a,b,*], Sylvie Yotte[b], Fazia Fouchal[b], Alaa Chateauneuf[c]

[a] Researcher, Algerian Government, Algerian Ministry of Defense, Tagarins 16000 Algiers, Algeria
[b] University of Limoges, Laboratory of Heterogeneous Material Research Group, Civil Engineering and Durability Team, Boulevard Jacques Derche, 19300, Egletons, France
[c] Clermont University, Blaise Pascal University, Institute Pascal, BP 10448, F-63000 Clermont-Ferrand, France

ARTICLE INFO

Article history:
Received 17 October 2015
Received in revised form
11 December 2015
Accepted 20 December 2015
Available online 28 December 2015

Keywords:
Bridge
Inspection
Defect
Probability
Masonry

ABSTRACT

This paper presents a methodology for probabilistic assessment of masonry vaults bearing capacity with the consideration of existing defects. A comprehensive methodology and software package have been developed and adapted to inspection requirements. First, the mechanical analysis model is explained and validated by showing a good compromise between computation time and accuracy. This compromise is required when probabilistic approach is considered, as it requires a large number of mechanical analysis runs. To model the defect, an inspection case is simulated by considering a segmental vault. As the inspection data is often insufficient, the defect position and size are considered to be unknown. As the NDT results could not provide useful and reliable information, it is therefore decided to take samples with the obligation to minimize as much as possible their number. In this case the main difficulty is to know on which segment the coring would be mostly efficient. To find out, all possible positions are studied with the consideration of one single core. Using probabilistic approaches, the distribution function of the critical load has been determined for each segment. The results allow to identify the best segment for vault inspection.

1. Introduction

Masonry arch bridges, still in service, represent more than 40% of bridges in Europe [1]. Most of them are century old and the degradation process is already running since several decades. Actually, the maintenance and repair continue to represent serious issues for their managers. Indeed, many repairs have been undertaken without ensuring the aimed durability. The question is: how to repair old masonry vaults while ensuring relevant actions that extend their service life? In fact, repair work is directly related to diagnosis. The more accurate the diagnosis is, the more durable and less expensive repairs are. Although several defects can be detected using non destructive tests (NDT), some defect are difficult, and sometimes impossible, to detect without coring [2]. The main difficulty is therefore to know where coring could be most efficient, in terms of information about the vault defects and the ultimate load capacity.

Several methods were developed since the fifteenth century to calculate masonry vaults, starting from the well-known empirical rules (see Table 1 in Ref. [3]). These rules allow to determine the main arch dimensions by mean of simple

* Corresponding author.
E-mail addresses: abdelmounaim.zanaz@etu.unilim.fr, zanazabdelmounaim@yahoo.fr (A. Zanaz), sylvie.yotte@unilim.fr (S. Yotte), fazia.fouchal@unilim.fr (F. Fouchal), alaa.chateauneuf@univ-bpclermont.fr (A. Chateauneuf).

http://dx.doi.org/10.1016/j.csse.2015.12.001

relationships developed by introducing experimentally obtained coefficients, sometimes depending on the used materials which have survived very long time in the absence of proper modeling theory. Several methods have been developed for the assessment of load-carrying capacity, such as Military Engineering experimental Establishment (MEXE) [4,5] and Railway Empirical Assessment Method (REAM) [6,7]. The first method allows the calculation of the allowable axle load on a bridge based on a so-called idealized axle load calculated with reference to an "ideal" bridge. The arch is assumed to be parabolic in shape with span/rise ratio of 4, compressive stress limit of 1400 kN/m^2, and tensile stress limit of 700 kN/m^2. This idealized axle load is then modified by factors allowing to consider the difference between the actual arch and the ideal one [8] such as the span/rise factor, the profile factor which takes into account the difference between the realistic arch line and a parabolic arch, depending on the arch rise at the haunches and the rise at the crown, the material factor depending on the material strength of the vault and filling material, the joint factor which takes into account the condition of the joint material and its thickness, and finally the condition factor which depends on the general arch condition in order to take into account the possible presence of cracks and/or deformations. The REAM method allows to obtain a preliminary arch assessment without calculations, by means of graphs for the determination of the required vault thickness based on a study conducted on different bridges with span ranging between 2 m and 25 m span/rise ratio lower than 8, filling depth above the crown between 25 cm and 150 cm and axle load is between 10 tons and 25 tons. The limit analysis method was adopted by Kooharian in 1953 for the study of arcs formed of segments [9]. The principle of this method is to determine the allowable loads under which the vault does not collapse. It is shown that if the thrust line is within the arc thickness, then the stability of the structure is guaranteed. The yield design methods [10,11] are derived from Heyman's studies on the yield design of masonry arches [12,13]. In 1976, Salençon provided the basis for this method and generalizes the limit analysis methods by replacing the perfect plasticity condition by a material strength criterion. Finally, the finite element method [14,15] and distinct element method [16] are currently considered as the main numerical methods for solving partial differential equations, through the development of computer technology. These methods are characterized by their high level of accuracy, but only when detailed input data are provided. Indeed, various software using 1D, 2D or 3D models have been developed, but most of them allow the analysis of structures without defect. In parallel, some authors have proposed methods for detecting defects [17–20]. Some others have proposed methods allowing to assess the load bearing capacity of damaged arches [1,21]. Generally, these methods provide the mechanical response assuming defect characteristics as known (position, depth, extent . . .etc.) after carrying out some ND tests, which is not always the case, and consequently destructive tests become necessary. In this framework, the present aims, in addition to assess the load bearing capacity of the vault, to identify on which segment the destructive test will be the most efficient, and presents a methodology for probabilistic assessment of the effect of defects, caused by water infiltration, on the vault bearing capacity.

One of the major reasons for building abandonment is the excessive cost of inspections and repairs, in addition to technical feasibility and reliability. Indeed, when an inspection is carried out, the observations and the assessment of the vault state are subject to large uncertainties. The vault thickness for example is an input data which is known with large uncertainties. The formulae given by Oliveira et al. [3] (in Table 1) has been used to determine this parameter and provide upper and lower bounds between which there is much disparity [24]. In addition, many of the existing bridges that were originally built for car traffic are currently being used for heavy traffic and even for trucks in some cases. From another point of view, the study of stone alterations revealed several material loss patterns and therefore changes in geometry of segments which are not visible, in most of the cases. This kind of situation requires a rigorous inspection program and associated predictive models. The first problem of the bridge owner is to know how much money he/she can spend for inspections. Depending on his/her budget allocation, the scope and extent of inspection can be defined, and consequently the uncertainties on inspection results will be high or not. The number of tests on materials, of in-situ measurements, and the NDT methods to be applied will depend on this choice. The majority of available methods for assessing the masonry vault behavior are deterministic. They can predict the load bearing capacity of the vault provided that all the variables involved in the mechanical response are assumed to be deterministic (i.e., perfectly known), which is not true because of the uncertainties involved in the geometry, materials,

Table 1
Geometrical, physical and mechanical characteristics of the studied vault.

Designation	Unit	Value
Span (s)	m	6.18
Rise (r)	m	2.50
Vault thickness (t)	m	0.58
Backfill depth above the crown (f)	m	0.85
Pavement thickness (e)	m	0.28
Segments unit weight	kN/m^3	24
Pavement unit weight	kN/m^3	21
Backfill unit weight	kN/m^3	18
Segments Young's modulus	GPa	48
Tensile resistance of segments	kN/m^2	0
Pavement Young's modulus	MPa	20
Backfill cohesion	kN/m^2	0
Backfill angle of shearing resistance	rad	$\pi/6$
Pavement angle of shearing resistance	rad	$\pi/6$

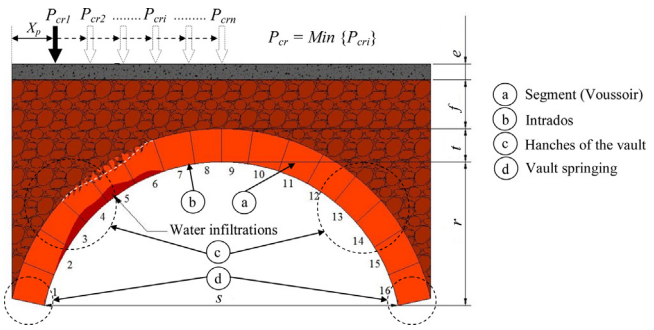

Fig. 1. Arch under consideration.

loads . . . etc. In recent years, the reliability-based assessment methods of structures have been developed. These methods take into account the uncertainties of the involved variables, by applying structural reliability methods, among them Monte Carlo simulations [22] are commonly applied in various engineering fields. Most of the applications have shown that large amount of money that can be saved by accurate and efficient assessment based on probabilistic approaches [23]. In this paper, Monte Carlo simulations are coupled with the finite element method and implemented in a software package (named ArcProg_Z), in order to propose a consistent methodology for probabilistic assessment of the load bearing capacity of the vault. This methodology aims at minimizing the number of measurements and consequently the diagnosis cost. The first part of this paper presents the model assumptions (loads, materials, etc) and the second part is devoted to the study of masonry vault inspection of localized defect. Finally, the probabilistic modeling of inspection is carried out and the results are discussed with respect to the vault assessment.

2. Arch model

It is well approved that water presence is critical for most of masonry alterations [26–28]. It is therefore mandatory to consider this effect for the load bearing capacity of masonry. The model proposed herein deals with the most encountered situation during inspections of old masonry structures, which is related to material losses mainly affecting limestone. Fig. 1 shows the analyzed arch configuration, including loading and defect. For simplicity, the study is limited to one localized defect (thickness loss of a number of segments); the extension to more defects is straight forward without difficulties. The vault is subjected to vertical loads due to its own weight, the filling material, and the axle load, as well as the associated horizontal pressure.

2.1. Model assumptions

The vault is modeled using beam finite elements representing the loaded arch, in order to analyze its instability. The load takes into account the axle load, permanent filler weight and soil action (Fig. 2). The latter is modeled by horizontal and vertical springs acting at each node and affected by stiffness coefficients (k_h and k_v) taking into account the backfill modulus and the contact surface related to each node. The spring stiffness is nil when the deformations have the effect to keep the structure away from the backfill.

The failure is characterized by the appearance of four successive hinges (three hinges when the system is symmetrical and loaded on the arch key). A hinge occurs when the application point of the stress resultant is outside the central third

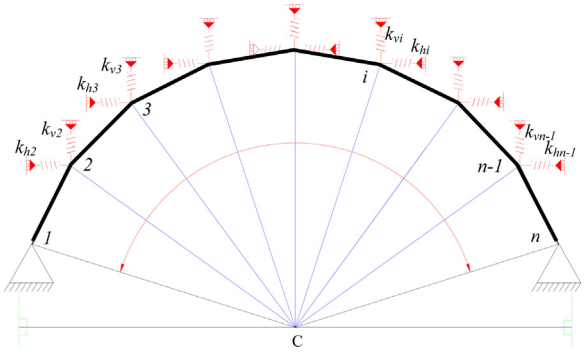

Fig. 2. Modeling of backfill reaction (ArcProg_Z).

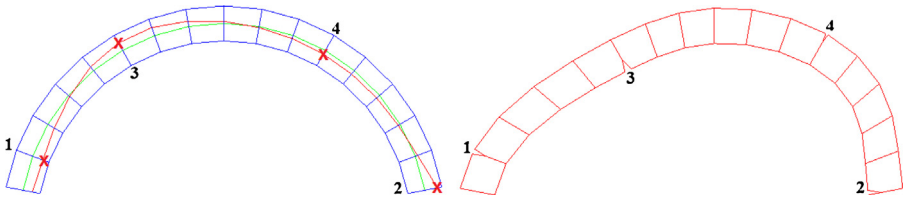

Fig. 3. Thrust line and failure mechanism (ArcProg_Z).

of the arch thickness i.e., no tensile stress can take place at the interface between segments, due to cracking (Fig. 3). This method gives a lower bound of the arch capacity, as it can sustain loads even beyond the first cracking.

The arch capacity computation procedure is illustrated in Fig. 4. In this procedure, the position of the load point is moved along the half-vault, with a constant steps Δx.

For each loading position, the incremental finite element analysis is performed. The applied load is increased by a steps Δp until the formation of four hinges corresponding to arch instability. The critical load is thus computed for the specified axle position. The procedure can thus be continued for other loading positions, in order to model the traffic over the bridge. The minimum value of the calculated critical load corresponding to the vault bearing capacity P_{cr} is then deduced, as well as the corresponding critical position X_{cr}.

2.2. Comparison with previous studies

In order to validate the numerical model, the comparison is carried out with published theoretical and experimental results. Schwarzwasserbrücke bridge (Switzerland) has been modeled with RING2 software [25]. With a span of 16.75 m and a rise of 2.84 m, this bridge is composed of 40 segments. The finite element analysis is performed by the program ArcProg_Z using bridge input data and the comparison is considered regarding the two main results: hinge locations and critical load. As a results, the four hinges were found to be exactly at the same positions and the critical load given by RING2.0 was 678.4 kN, which is very close to the one given by ArcProg_Z equal to 679.3 kN (i.e., the difference is around 0.1%).

The experimental results provide an interesting case-study for comparison. Shinafoot Bridge (UK) has been tested until failure [25]. It was composed of 11 segments with a span of 6.16 m and a rise of 0.83 m. Both critical load and hinge locations have been recorded. ArcProg_Z critical load differs by only 3.6% from the experimental result and the four hinges were also located at the same positions.

From these comparisons, the accuracy of the developed numerical model has been shown, allowing its validation to predict the arch bearing capacity. An interesting compromise is found between computation time and accuracy, which allowed using a probabilistic approach, to perform a large number of analyzes in a reasonable time span.

2.3. Defect modeling

For modeling purpose, it is assumed that the defect extent is a function of its maximum depth. For simplification reasons, all segments are assumed to have the same Young's modulus. The defect is characterized in the following way: the position of the maximum depth of the defect is defined by the distance from the left end of the vault, noted X_d as indicated in Fig. 5. To study the effect of the defect position on the arch bearing capacity, the defect width is projected on the horizontal axis ($l = l_l + l_r$) and located with respect to X_d such that ⅓ of this length noted l_r is located at the right of X_d and the remaining length l_l at the left side. The horizontal shift of this interval along the half-span allows to have more segments affected by the defect when approaching the support and fewer segments when approaching the arch key, as shown in Fig. 6. This allows characterizing the unsymmetrical material losses caused by water infiltrations taking into account the effect of gravity, which leads to greater flow on the left part of the defect than on the right of the position X_d. It is to note that this configuration is given for a defect at the left of the arch key. When the defect is located at the right of the arch key, its geometry can be symmetrically generated with respect to the mid-span vertical axis, as water flows to the right. The particular case where the defect is located at the arch key imposes similar flows in both sides of the key ($l_l = l_r$), and in this case the defect becomes itself symmetrical. The defect length ($l_l + l_r$) is linked to the capacity of the liquid to flow along the arch surface. Therefore, it depends on the porosity and the stratification of the stones.

In order to predict on which segment the measurement should be performed, coring in each segment composing half of the vault is simulated. The defect depth, noted h_m, is measured. It should be emphasized that it is not possible to determine this measurement before analyzing the sample in the laboratory and determining the healthy thickness of the measured segments. The measurement position noted X_m is determined by assuming that coring is carried out in the middle of each segment. The uncertainty on X_m is related to the fact that the measurement is localized and it is estimated that this loss of thickness in a given location indicates a material loss at the measurement vicinity.

As material losses due to water actions are assumed to be smooth, the defect distribution is modeled by a four-degree polynomials on the right and on the left side of the maximum depth location. To determine the polynomial coefficients, the

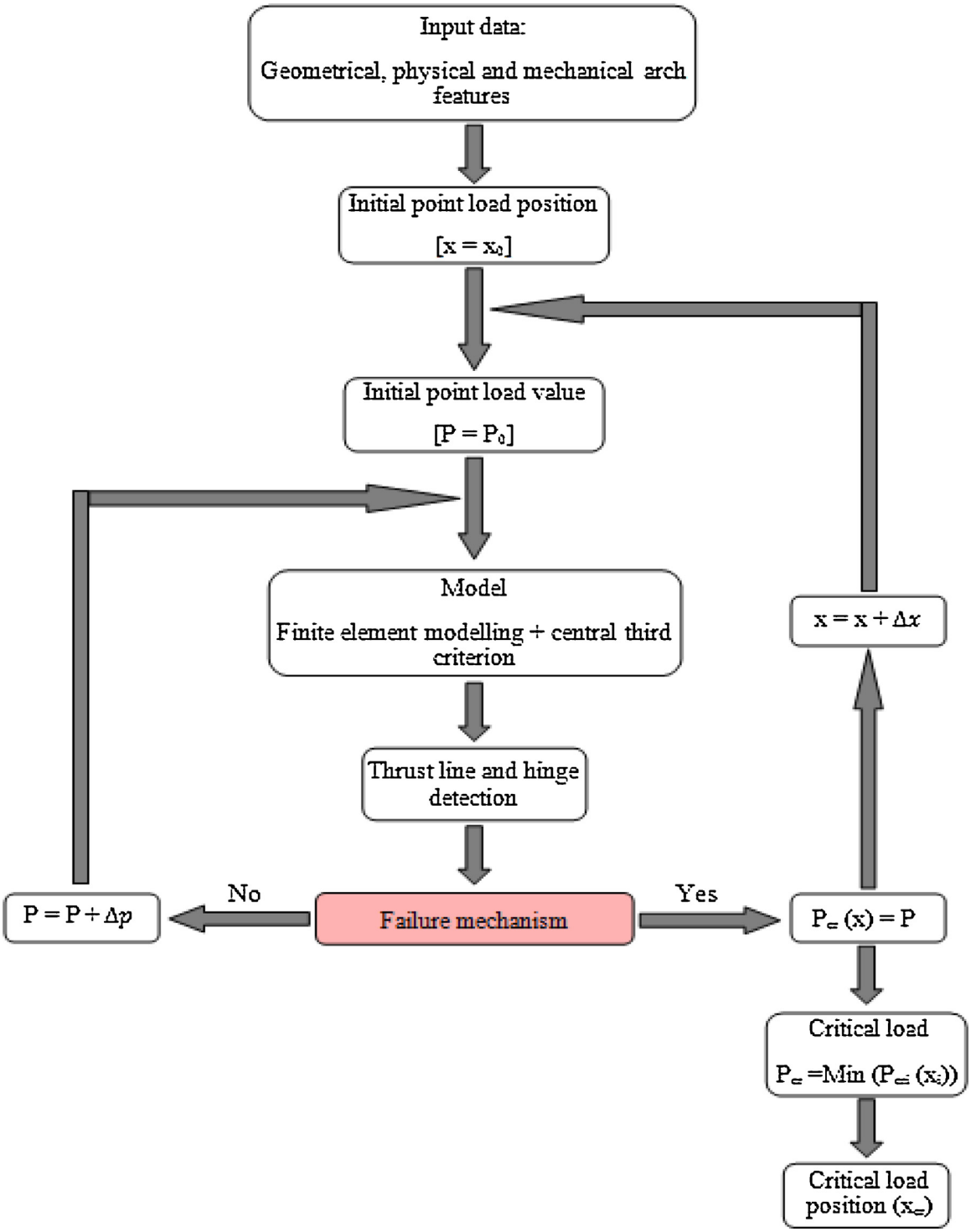

Fig. 4. Schematic calculation procedure (ArcProg.Z).

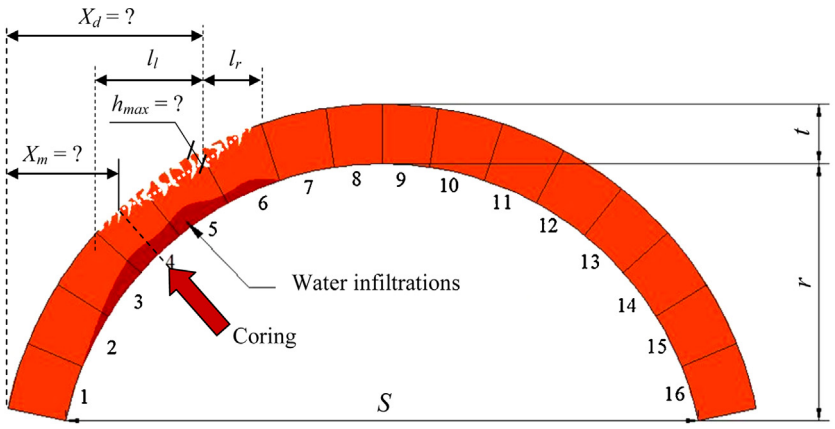

Fig. 5. Defect modeling and parameters (step 1).

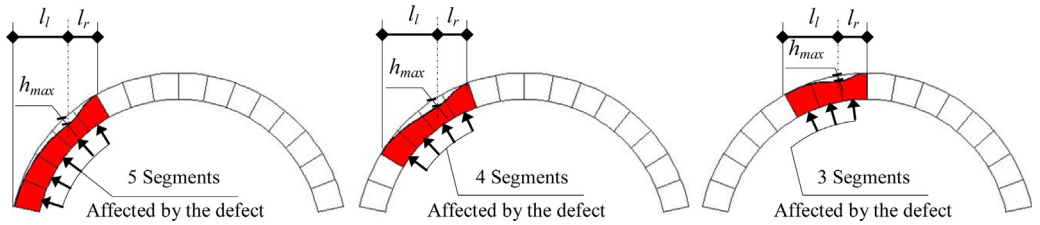

Fig. 6. Number of segments affected by the defect depending to the defect position.

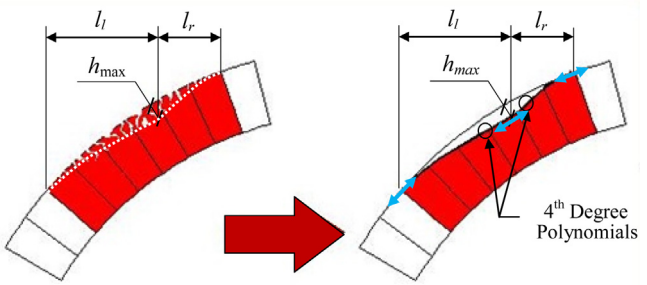

Fig. 7. Defect modeling (step 2).

geometrical conditions are imposed by considering slope continuities between the two curves, and between the defect ends and the unaffected part of the vault, as shown in Fig. 7.

In the numerical analysis, the thickness of a segment is assumed constant and the outer surface of the segment bottom is considered as that of the segment. From the above conditions, the polynomial functions can be described by the following relationships, for left and right parts of the defect, respectively.

$$\begin{cases} h_{dl}(X) = h_{max}(X - (X_d - l_l))^2 (X - (X_d + l_l))^2 \\ h_{dr}(X) = \alpha h_{max}(X - (X_d - l_r))^2 (X - (X_d + l_r))^2 \end{cases} \quad (1)$$

In these relationships, h_{dr} and h_{dl} are respectively the defect depths at the right and the left of the maximum defect depth, noted h_{max}. The remaining thickness of the segment in the defect zone is then deduced by the relationships (2), indicating the position of the defect at the right or at the left depending on the position of the measurement.

$$\begin{cases} h_{vl} = h_{hv} - h_{dl} = h_{hv} - h_{max}(X - (X_d - l_l))^2 (X - (X_d + l_l))^2 \\ h_{vr} = h_{hv} - h_{dr} = h_{hv} - \alpha h_{max}(X - (X_d - l_r))^2 (X - (X_d + l_r))^2 \end{cases} \quad (2)$$

By removing the defect depth, which is depending on h_{max} and X_d, from the vault thickness, the developed program determines the position and the number of segments that have suffered material losses. The program will then modify the thicknesses of affected segments and computes the mechanical response (Fig. 8).

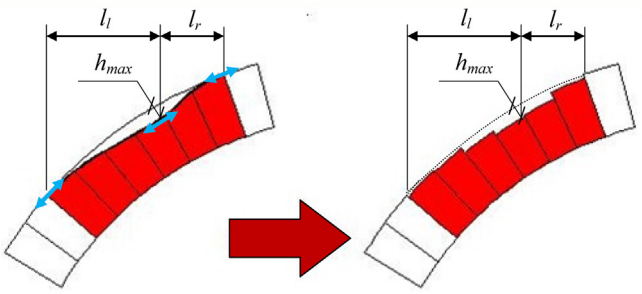

Fig. 8. Discretization of the defect model (step 3).

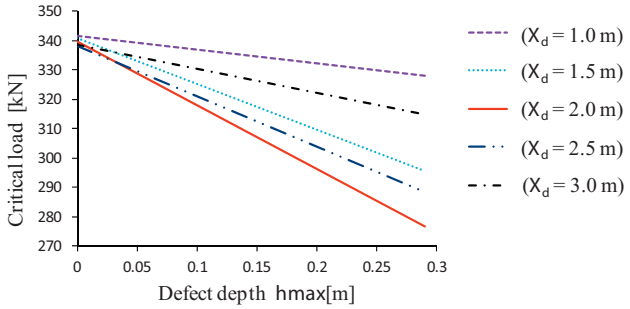

Fig. 9. Critical load depending on defect depth.

3. Inspection situation

The considered inspection situation for masonry bridges corresponds to the case of water infiltrations which are assumed to be observed on the left side of the vault intrados (the concave curve of the vault). These water infiltrations might indicate the existence of a vault defect. The remaining thickness of the concerned segment and/or of the adjacent ones, the defect extent, its maximum depth and its position are uncertain parameters.

The evaluation of test methods with respect to their applicability for the assessment of masonry arch bridges was carried out by Oliveira et al. [2]. It shows that the only method that can provide useful and reliable information on this type of defect is coring, and that ground penetrating radar, sonic methods and conductivity measurement cannot provide sufficiently reliable information. However, before taking any sample, it is necessary to address two important questions: where the coring should be carried out? And how many cores? For the majority of the cases, it is impossible to answer accurately these questions, which often involves to consider additional samples and consequently, additional costs. Using probabilistic approaches, the aim of this study is to address the first question by considering the case where one single core is carried out.

3.1. Influence of defect depth variation

The analyzed vault consists of 16 limestone segments whose geometrical, physical and mechanical characteristics are summarized in Table 1. The applied traffic load which causes collapse is sought, as a function of defect conditions.

The measured defect depth, noted h_m, taken into account in the numerical application is 0.02 m. At first, the study is limited to the five defect positions shown in Table 2 with a step of 0.50 m to simulate the defect position X_d along the half-vault. For each location, various losses of thickness are considered. The steps of 0.25 m and 5 kN are fixed for respectively the point load position X_p and the load magnitude.

For different values of defect location X_d, Fig. 9 shows the critical traffic load as a function of the defect depth. These results show that, for the same defect location X_d, the thickness loss and the critical load are correlated and a linear relationship

Table 2
Defect parameters.

Designation	X_d	l_r	l_f	h_m
Values [m]	1.0 1.5 2.0 2.5 3.0	0.5	1.0	0.02

Table 3
Quantification of error on slopes.

Xd[m]	Slope value		Error [%]
	Calculation	Polynomial	
1.00	−45.876	−44.73	2.56
1.50	−156.1	−161.87	3.70
2.00	−217.28	−206.83	5.05
2.50	−171.47	−179.61	4.75
3.00	−82.564	−80.21	2.93

can be drawn. For nil thickness loss, all the results tend to the same point, corresponding to the critical load for arch without defect. With the increase of thickness losses, the rate of load capacity reduction is shown to be strongly depending on the defect location.

The general equation of the load bearing capacity in terms of defect depth can be written as:

$$P_{cr=\alpha(X_d)}.h_{max} + P_{cr0} \tag{3}$$

where P_{cr} is the critical load, α is the slope (i.e., rate of capacity decrease) and P_{cr0} is the critical load for vault without defect.

To express the slope α depending on the maximum defect position X_d, a polynomial of second degree is adopted and evaluated by regression as following:

$$\alpha(X_d) = 144.36X_d^2 - 595.18X_d + 406.09 \tag{4}$$

The comparison of the slopes of several straight lines using Eq. (4) shows a good approximation of the reference values; the maximum error is about 5% (Table 3).

3.2. *Influence of defect position*

In the course of inspection, the vault thickness measurement is carried out. In the case of a unique measurement on the arch, the location of the maximum defect thickness is unknown; it is therefore necessary to study every possible location. For a measurement carried out at a distance X_m from the left support, the measured thickness can be either at the left ($X_m < X_d$) or at the right ($X_m > X_d$) of the maximum defect depth h_{max}; a special case can be met when the measured thickness is located at the maximum defect position ($X_m = X_d$). It is also assumed that when the thickness loss is greater than half the original thickness of the segment, the defect location would be visible on the vault intrados. It means that, the defects that have reached this size are directly identified during visual inspection and are out of the scope of the present study. The first step is to determine the maximum value of defect thickness depending on its position X_d, according to the measured thickness h_m. A thickness loss h_m measured on a core at the position X_m may thus correspond to any left-side position X_{ml} or right-side position X_{mr} of the defect, as shown in Fig. 10. To find the critical load corresponding to this measurement, it is necessary to deduct the maximum defect depth h_{max}, the defect location and the number of segments affected by the defect. Under these

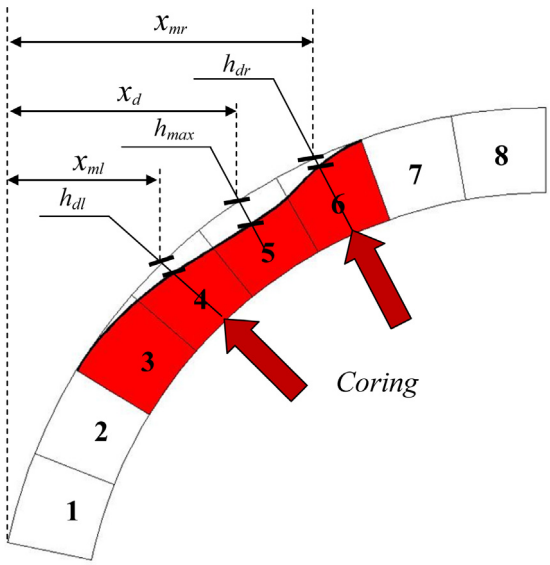

Fig. 10. Relative position of the defect and the measurement point.

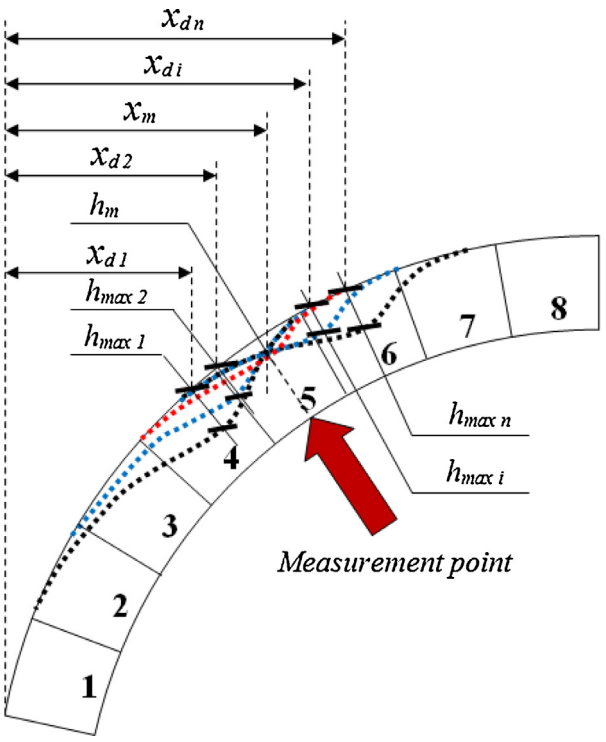

Fig. 11. Possible defect locations X_d corresponding to the same measurement point X_m.

considerations, a measurement point corresponds to several couples (X_d, h_{max}) according to the Relationship (5). It is found that h_{max} depends only on X_d and the parameters l_l and l_r. The associated relationship giving h_{max} can be obtained when the measurement point is located at either the left or the right of the maximum defect depth. For a given measurement point X_m, Eq. (1) gives a relation between h_{max} and X_d. h_{max} can be then deduced for right and left positions through the Relationship (5), as a function of the known position of the measured point X_m and the unknown position of defect X_d.

$$\begin{cases} h_{max} = \dfrac{h_{dl}}{(X_m - (X_d - l_l))^2 (X_m - (X_d + l_l))^2} \\ h_{max} = \dfrac{h_{dr}}{\alpha (X_m - (X_d - l_r))^2 (X_m - (X_d + l_l))^2} \end{cases} \tag{5}$$

Fig. 11 shows the various possibilities for a given measurement data (X_m, h_m). It can be clearly seen that a measurement output (X_m, h_m) leads to different possibilities (X_{di}, h_{maxi}), which are assumed to be identically probable (as no other information is available, to induce preferential assessment). In other words, a large range of defect location and maximum depth can be associated to each measured vault thickness h_m at a given location X_m. As each defect configuration (X_d, h_{max}) corresponds to different critical load, the measurement output will lead to a probability distribution function for the load bearing capacity of the vault.

For each value of the defect location X_d, a critical load is deduced by finite element analysis, as described in the above section. For each measurement position X_m, the curve giving the critical load as function of the defect location X_d can be plotted. For the six segments of the left half of the vault (segments 2–7), Fig. 12 gives the obtained critical load curves when the measured material loss is given as $h_m = 0.02$ m.

The boundaries on the left and right of these curves are related to the imposed maximum defect size h_{max}. It is assumed that this maximum size cannot exceed half of the segment thickness when the intrados surface is intact. Furthermore, it is worth recalling that the measurement position, noted X_m, is determined by assuming that coring is carried out in the middle of each segment. For each possible defect location, the maximum defect depth is determined. The results show that, for segments 2 and 3 (Fig. 12(a) and 12(b) respectively), the lowest load bearing capacity corresponds to the case where the maximum defect is on the left side of the measurement point X_m, i.e., on the springing zone (i.e., supports zone). For segments 4 and 5 (Fig. 12(c) and (d)), in contrast to the two previously mentioned segments, the lowest load bearing capacity is obtained with maximum defect located at the right of X_m, which corresponds to the haunches of the vault (parts of the vault where the stresses are the most significant, generally located at half vault rise). The segment number 6 (Fig. 12(e) gives almost the same value of the load bearing capacity, either on the left or on the right. In this case, the vault bearing capacity is strongly related to the measurement value h_m. Finally, with regard to the seventh segment (Fig. 12(f)), the lowest load

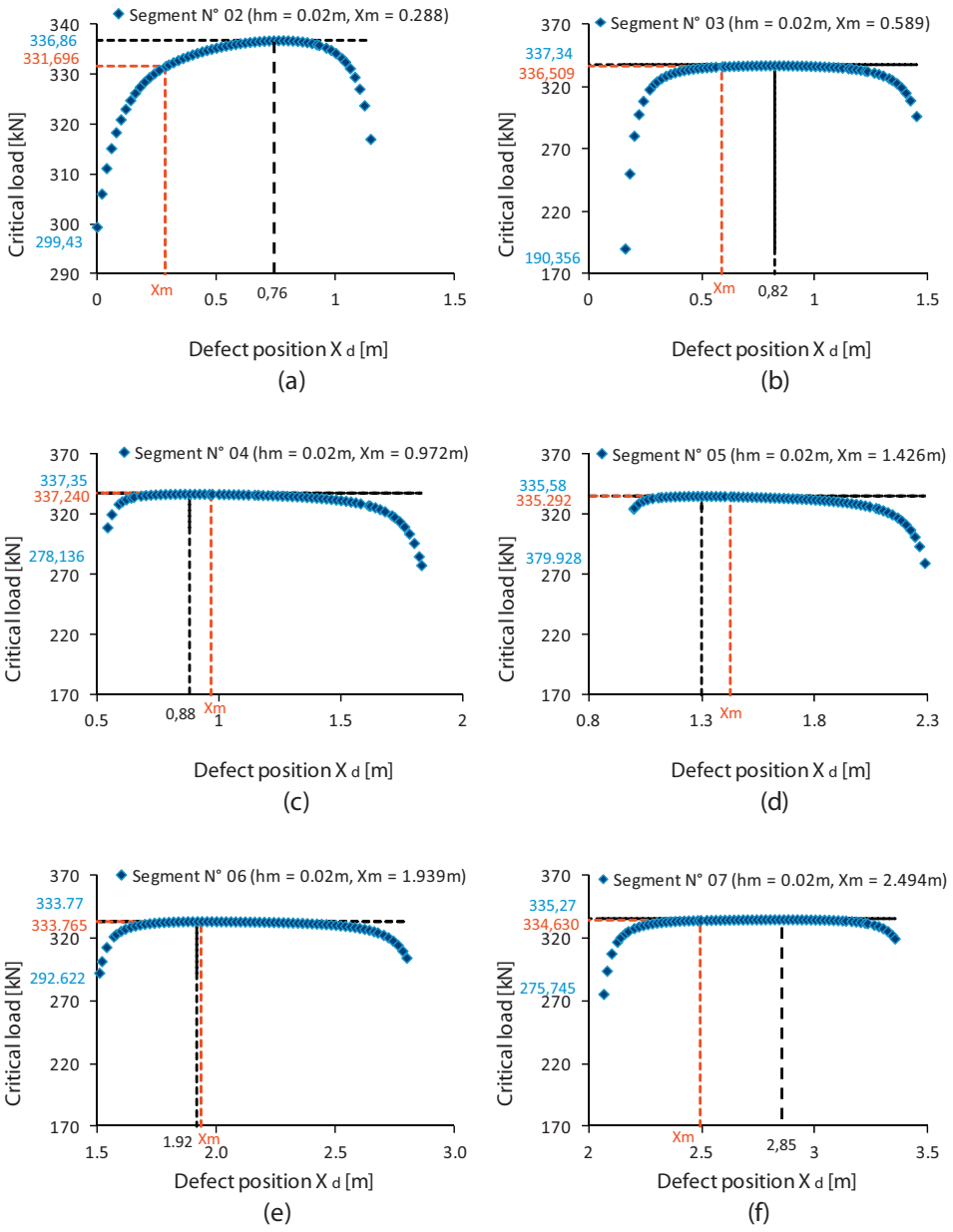

Fig. 12. Critical load depending on defect position for the tested segments.

bearing capacity is again obtained with the maximum defect located at the left of X_m, i.e., haunches of the vault. All this makes it possible to identify two vault zones where the presence of a defect leads to the greater losses in the vault bearing capacity. These zones are classified according to their degree of influence, which are firstly the vault springing (i.e., supports of the vault) then the haunches. Among the six tested segments, it is the segment number 3 which gives the lowest critical load (190.4 kN). The same analysis could also be applied to the other figures.

Fig. 12(b) considers the case of a sampling (X_m, h_m) carried out in the middle of segment 3 ($X_m = 0.589$ m and $h_m = 0.02$ m). According to the prescribed model, the defect is located in the interval $I = [0.589 - 0.5; 0.589 + 1.0]$. In addition, the limit on h_{max} (less than half of the segment thickness) allows to tighten the generated interval to [0.16; 1.23]. In this interval of X_d, the critical load P_{cr} ranges from 190 kN to 337 kN. If the defect was located in X_m, then the critical load value will be 336 kN. In fact, for each tested segment, the maximum value is obtained for a defect localized on the segment where the measurement is carried out. This is because the measured material loss will directly give the maximum depth of the defect. The farther the defect is from the measurement point, the greater is its maximum depth h_{max}, and the lower is the critical load. Knowing that the greatest length l_l or l_r does not exceed 2 segment lengths, the lower loads bearing capacities correspond to defects

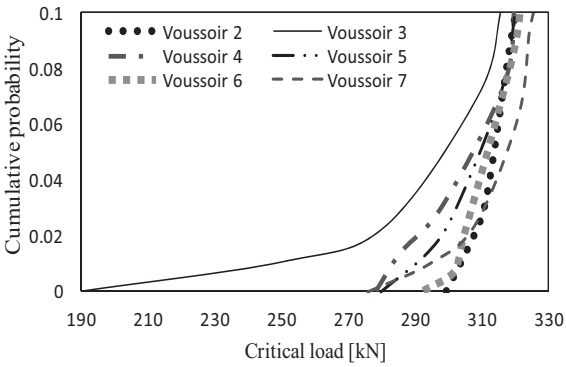

Fig. 13. Extreme values of obtained distribution functions (h_m = 0.02 m).

Table 4
Characteristic values of the obtained distributions.

	Segment number					
	2	3	4	5	6	7
Min	299	190	278	280	293	276
Max	337	337	337	336	334	335
1%	304	247	283	290	303	294
5%	315	297	310	310	313	320
10%	320	315	319	320	321	325

on the segments adjacent to the measurement point. So, repairs should be carried out not only on the measured segment, but also on the adjacent segments, because a defect on these segments leads to a lower critical load.

As all values X_d belonging to the interval I are equiprobable, the curves in Fig. 12 show the shapes of the probability density function of the critical load $p(P_{cr})$ conditioned by the measurement positions X_m. It is to note that the analysis was carried out with the measured material loss h_m = 0.02 m. The computation of the probability density on the interval $I = [X_{dmin}; X_{dmax}]$ is performed through numerical integration of $P_{cr}(X_d)$ values, by using Monte Carlo simulations. The shape of the density function depends strongly on the measured point, and implicitly on the possible defect location.

Fig. 13 shows the lower extreme values (i.e., less than 10% quantile) of the predicted capacity in terms of the defect position. For example, in the case of the segment number 3, a load less than 300 kN has 5% probability to be critical and represents 75% of the critical load range [190; 337 kN]. Considering that maximum defect depth is located at the measured point, the actual critical load is 336 kN, the critical load at 5% is 300 kN, and the error on the critical load is 11%. The greatest range corresponds to that of segment 3. Given the model and the shape of the vault, this corresponds to the measurement point that gives the largest number of segments on which the maximum defect can be located.

For all segments, the maximum value of the critical load is about 336 kN. The difference lies in the minimum values and the percentiles in the lower extreme values. Table 4 gives some characteristic values of these distributions. The 10% percentile interval is very close and ranges between 315 kN and 325 kN. It means that if we take a risk of about 10% of error on X_d, the critical load regardless which segment is measured, will be greater than 315 kN.

As a reminder, the addressed issue in the beginning of this study was to know on which segment coring would be the most efficient in order to minimize the number of measurements? The analyse of these values reveals that carrying out measurement on the segment 3 leads to a critical load which may be exceeded in only 1% of defect locations, and still remain lower than the same measurement carried out on the other segments. It means that segment 3 is the best option that can be given to address this question. In the case where the measured material loss h_m is nil, there will be two possibilities: either the vault does not contain any defect, or there is a defect but located far from the measurement point. In the later case, the defect could be at more than 1 m on the right or 0.5 m on the left of the measurement point, according to the model assumptions. In order to confirm the most probable trend, another coring should be performed and the same methodology could be applied.

4. Conclusions

An effective probabilistic methodology, aiming to assess the load bearing capacity of damaged masonry vault, is proposed. In the case where the non destructive tests (NDT) cannot provide useful information about the defect, it allows knowing on which segment the coring will be more efficient, which minimizes considerably the number of cores and consequently the diagnosis cost.

The consequence of defect on the load bearing capacity of the vault is simulated. A diagnosis case-study is provided by considering the thickness loss caused by water infiltrations. The defect is modeled through three steps: First, the defect extent is assumed as a function of its position in order to consider the effect of gravity. Then, the shape of the defect is approximated by two four-degree polynomials: one on the right and one on the left of the maximum defect location. They are determined by considering slope continuities between the two curves, and between the defect ends and the rest of the vault. Finally, the projection of the defect curve, given by the two polynomials, on the vault thickness is performed and the developed program determines the position and the number of segments that have suffered losses, modifies respectively their thicknesses and computes the mechanical response. Monte Carlo simulations allow to obtain the distribution function of the critical load, which is determined for each segment. The analysis of the obtained distributions allowed identifying the searched segment. It corresponds to the segment which has the largest interval of critical load variation. In fact, for all segments, the maximum values of the critical load are very close, the minimum values and the percentiles in the low extreme values are the varying item. Finally, knowing the critical load distributions for other thickness loss values will allow a finer diagnosis strategy.

Acknowledgements

The authors present their acknowledgements to Algerian government in general and to Ministry of Defence in particular for interest they have kindly given to this research work and their support.

References

[1] T. Kamiński, J. Bień, Application of kinematic method and FEM in analysis of ultimate load bearing capacity of damaged masonry arch bridges, Procedia Eng. 57 (2013) 524–532.
[2] Z. Orbán, M. Gutermann, Assessment of masonry arch railway bridges using non-destructive in-situ testing methods, Eng. Struct. 31 (10 October) (2009) 2287–2298.
[3] D.V. Oliveira, P.B. Lourenço, C. Lemos, Geometric issues and ultimate load capacity of masonry arch bridges from the northwest Iberian Peninsula, Eng. Struct. 32 (12 December) (2010) 3955–3965.
[4] PIPPARD A. J. S., A study of the Voussoir arch, His Majesty's stationery Office, National Building Studies, Research Paper n°11, 52p., 1951.
[5] Christchurch, MEXE. Military Engineering experimental Establishment. «Military load classification of civil bridges by reconnaissance and correlation methods», 1963.
[6] J.C. Trautwine, Civil Engineer's Pocket-Book, New York Wiley Publisher, 1871, pp. 770, 1871.
[7] Harvey, Rule of thumb method for the assessment of arches. Rapport UIC, draft, 2007, pp. 22, 2007.
[8] Design manual for roads and bridges., vol. 3. Highway structures - inspection and maintenance, Section 4: Assessment, BA16/97, 2001.
[9] Kooharian, Limit Analysis of Voussoir (Segmental) and Concrete Arches, Journal of the American Concrete Institute 317-328, V. 24, N° 4, Dec. 1952, Proceedings V. 49., 1953.
[10] W.E.J. Harvey, Application of the mechanism analysis to masonry arches, Struct. Eng. 66 (5) (1988) 77–84.
[11] P. Buhan, R. Mangiavacchi, R. Nova, G. Pellegrini, J. Salencon, Yield design of reinforced earth walls by a homogenization method, J. Geotech. 39 (2) (1989) 189–201.
[12] J. Heyman, The stone skeleton, Int J. Solides Struct. 2 (1966) 269–279.
[13] J. Heyman, The safety of masonry arches, Int. J. Mech. Sci. 11 (1969) 363–385.
[14] B.G. Galerkin, Développement en série des solutions de quelques problèmes d'équilibre élastique des poutres et des plaques, VestnikInzhenerovi Tekhnikov 19 (1915) 897–908.
[15] O.C. Zienkiewicz, Y.K. Cheung, The Finite Element Method in Structural and Continuum Mechanics, McGraw-Hill Book Company, 1967, 2015, pp. 272.
[16] Cundall, A computer model for simulating progressive large-scale movements in blocky rock system, in: Proceedings of the Symposium of the International Society for Rock Mechanics, vol. I. Nancy, France, n.II-8 (1971), Nancy, France, 1971.
[17] L. Binda, A. Saisi, C. Tiraboschi, S. Valle, C. Colla, M. Forde, Application of sonic and radar tests on the piers and walls of the Cathedral of Noto, Constr. Build. Mater. 17 (8 December) (2003) 613–627.
[18] L.F. Ramos, G. De Roeck, P.B. Lourenço, A. Campos-Costa, Damage identification on arched masonry structures using ambient and random impact vibrations, Eng. Struct. 32 (1 January) (2010) 146–162.
[19] R. Skłodowski, M. Drdácký, M. Skłodowski, Identifying subsurface detachment defects by acoustic tracing, NDT E Int. 56 (2013) 56–64, June.
[20] F. Bastianini, A. Di Tommaso, G. Pascale, Ultrasonic non-destructive assessment of bonding defects in composite structural strengthenings, Compos. Struct. 53 (4 September) (2001) 463–467.
[21] N. Domede, A. Sellier, T. Stablon, Structural analysis of a multi-span railway masonry bridge combining in situ observations, laboratory tests and damage modelling, Eng. Struct. 56 (2013) 837–849, November.
[22] K.-H. Ng, C.A. Fairfield, Monte Carlo simulation for arch bridge assessment, Constr. Build. Mater. 16 (5 July) (2002) 271–280.
[23] J.R. Casas, Reliability-based assessment of masonry arch bridges, Constr. Build. Mater. 25 (4 April) (2011) 1621–1631.
[24] I. de Arteaga, P. Morer, The effect of geometry on the structural capacity of masonry arch bridges, Constr. Build. Mater. 34 (2012) 97–106, September.
[25] ICOMOS-ISCS, Illustrated glossary on stone deterioration patterns. International Council On Monuments and Sites, International Scientific Commitee for Stone, 2008, pp. 86, 2008.
[26] E. Vejmelková, M. Keppert, Z. Keršner, P. Rovnaníková, R. Černý, Mechanical, fracture-mechanical, hydric, thermal, and durability properties of lime-metakaolin plasters for renovation of historical buildings, Constr. Build. Mater. 31 (2012) 22–28, June.
[27] T. Poli, L. Toniolo, M. Valentini, G. Bizzaro, R. Melzi, F. Tedoldi, G. Cannazza, A portable NMR device for the evaluation of water presence in building materials, J. Cult. Herit. 8 (2 April) (2007) 134–140.
[28] Alix GRANDJEAN, Capacité portante de ponts en arc en maçonnerie de pierre naturelle—Modèle d'évaluation intégrant le niveau d'endommagement, Thèse, École Polytechnique Fédérale De Lausanne, Lausanne-suisse, 2009.